Progress In Electromagnetics Research Letters, Vol. 81, 29–37, 2019

A Compact Dual-Band Metamaterial Inspired Antenna with Virtual Ground Plane for WiMAX and Satellite Applications

Ashish Gupta*, Abhipsha Patro, Akanksha Negi, and Arpit Kapoor

Abstract—A compact dual-band metamaterial-inspired antenna is designed and developed in this paper. This design is carried out by loading a stub (acts as virtual ground plane) onto a circular microstrip fed patch antenna. The proposed antenna resonates at two frequencies $f_{c1} = 2.70\,\text{GHz}$ and $f_{c2} = 7.34\,\text{GHz}$ with $-10\,\text{dB}$ simulated impedance bandwidth of 6.6% (2.62–2.80 GHz) and 14.57% (6.57–7.65 GHz), respectively. First band is due to the metamaterial transmission line while second band is due to the coupling between microstrip feed and ground plane. Electrical size of the proposed antenna is $0.27\lambda_0 \times 0.27\lambda_0 \times 0.014\lambda_0$, where λ_0 is the free space wavelength at $f_0 = 2.70\,\text{GHz}$. In addition, this antenna provides antenna gain of 1.49 dB at 2.70 GHz and 3.23 dB at 7.34 GHz in the boresight direction. This antenna also provides dipolar type pattern in the xz plane whereas omnidirectional pattern in the yz plane with cross polarization level of $-32\,\text{dB}$ in the lower band while cross polarization level of $-23\,\text{dB}$ is maintained even in higher band. The proposed antenna's compactness, excellent radiation characteristics and ease of fabrication make it feasible to be utilized for Worldwide interoperability for microwave access (WiMAX) and satellite TV applications.

1. INTRODUCTION

In the current scenario multiband antennas are very important as they can be used for different applications [1, 2]. Essentially these antennas are to be integrated with devices such as mobile phones, laptops, Bluetooth, modem, and Zigbee [3, 4]. Enormous new devices are trending in the market such as wireless headphones, remote controls, wireless keyboard, and biomedical devices, in the present scenario, which challenges antenna engineers to meet their requirements. Metamaterial antennas are emerging as a big candidate in modern wireless communication as they offer multiband, wideband, beamforming, high gain features along with compactness [5–8]. These mentioned characteristics can be exploited using outstanding properties of metamaterials such as negative refractive index, zeroth order propagation and antiparallel group and phase velocity [9]. Zeroth order resonance is the phenomenon in which resonant frequency is independent from physical size of the antenna; therefore, it is responsible for miniaturizing the size of the antenna [10]. This phenomenon is exploited by many researchers, and subsequently ZOR antennas have been reported in the last decades [11, 12]. Lai et al. demonstrated that the number of resonant modes is proportional to different numbers of unit cells [11]. This concept motivates antenna designers towards working on multiband metamaterial antennas while maintaining compactness as one can have different bands by only adding unit cells, which are much smaller in size. Niu et al. presented a CPW-fed antenna with three unit cells to achieve multibands and later on converted it into wideband antenna by mode merging [13]. Multibands are usually originated due to coupling between different elements and by metamaterial (MTM) loading [14, 15]. Amani et al. proposed a tri-band antenna by loading CRLH transmission line into the structure [14]. In another work, MTM loading is used to achieve

Received 6 November 2018, Accepted 14 December 2018, Scheduled 7 January 2019
* Corresponding author: Ashish Gupta (ashish.gupta@jiit.ac.in).
The authors are with the Department of Electronics and Communication Engineering, Jaypee Institute of Information Technology, Noida, India.

multibands [15]. It has been observed that an additional band is originated due to MTM loading which can be tuned easily and independently. These additional modes/bands may suffer from low or negative gain problem in the case of zeroth order mode or lower modes [14]. These low gain problems are further overcome by using electromagnetic bandgap structures which suppresses the surface waves, and gain enhancement can be achieved [16]. Another technique to enhance the antenna gain is to loading an MTM unit cell superstrate onto the antenna. To carry out this scheme one has to design an MTM unit cell for the specified frequency band for which gain is deteriorated. This scheme has been successfully adopted by Li et al. in [17].

In this paper, a compact dual-band MTM antenna is designed and developed. In order to achieve an additional band, a metamaterial transmission line is realized. To do this a radial stub is introduced on the back side of the antenna structure. A meandered line inductor is connected between partial ground plane and radial stubs, to model the shunt inductance for so called composite right/left handed transmission line. Thus the proposed antenna has the first band from 2.62 GHz to 2.80 GHz with 6.6% fractional bandwidth at $f_{c1} = 2.70$ GHz. Another band is found from 6.57 to 7.65 GHz equivalent to 14.57% fractional bandwidth at $f_{c2} = 7.34$ GHz. In addition, a reasonable gain of 1.49 dB is maintained at lower band. Due to this, electrical size of antenna is $0.27\lambda_0 \times 0.27\lambda_0 \times 0.014\lambda_0$, where λ_0 is the free space wavelength at $f_0 = 2.70$ GHz.

2. ANTENNA GEOMETRY

Figure 1(a) shows the perspective view of the proposed antenna in which all the elements are displayed. Figs. 1(b) and (c) show the top and bottom views of the proposed antenna with optimized design dimensions of the antenna. This antenna comprises a circular patch split by a thin gap.

On the bottom side of the antenna, a partial ground plane is employed. It also has one radial stub which is connected to the partial ground plane via meandered line inductor. The antenna is fabricated on an FR4 Glass epoxy substrate ($\varepsilon_r = 4.4$, $\tan\delta = 0.02$) with 1.6 mm thickness. An equivalent circuit diagram of proposed antenna based on CRLH transmission line is shown in Fig. 1(d). Its modeling is described in the next section.

3. ANTENNA DESIGN AND ANALYSIS

The proposed antenna is designed and developed to realize the CRLH transmission line. To do this first 50 Ω feed line is implemented to have power flow to the circular patch. This feed line has magnetic flux which can be characterized by series inductance (L_R). It has been well recognized that any gap in between patch or signal line offers the series capacitance (C_L) [18]. Therefore, gap (C_g) plays a role of series capacitance in the transmission line. In order to characterize this series capacitance C_L, a gap is intended by splitting circular patch in this structure. It is evident by the previous studies that left handed inductance L_L is characterized by the current flow between patch and ground plane. In this structure, shunt inductance has been produced by a meandered line inductor which connects the partial ground plane and virtual ground plane. In this structure, a radial stub acts as virtual ground plane as it offers high capacitance and is shorted at high frequency. The gap between partial ground plane and virtual ground plane is associated with right handed capacitance C_R. This capacitance also consists of voltage gradient between patch and partial ground plane which can be characterized by C_C and is shown in Figure 1(d).

In order to see the behavior of input reflection coefficient with respect to different elements employed, the proposed antenna is designed and simulated for three different configurations as shown in Fig. 2. Primarily, a microstrip antenna is designed with a series gap C_g and named as Config-I. Further, to see the characteristics of metamaterial, meandered line inductor and radial stubs are integrated, but at the same time series gaps are removed. This configuration is named as Config-II whereas Config-III is represented as the proposed antenna. It can be observed from Fig. 2 that Config-I offers only one mode at 7.6 GHz which is due to coupling between feed and ground plane. Config-II is the manifestation of epsilon negative transmission line (ENG-TL), where series gap is not present. This originates another mode at 2.54 GHz due to implementation of ENG-TL which shows metamaterial behavior; however, power does not propagate particularly at this frequency. In addition, the second band is extended from

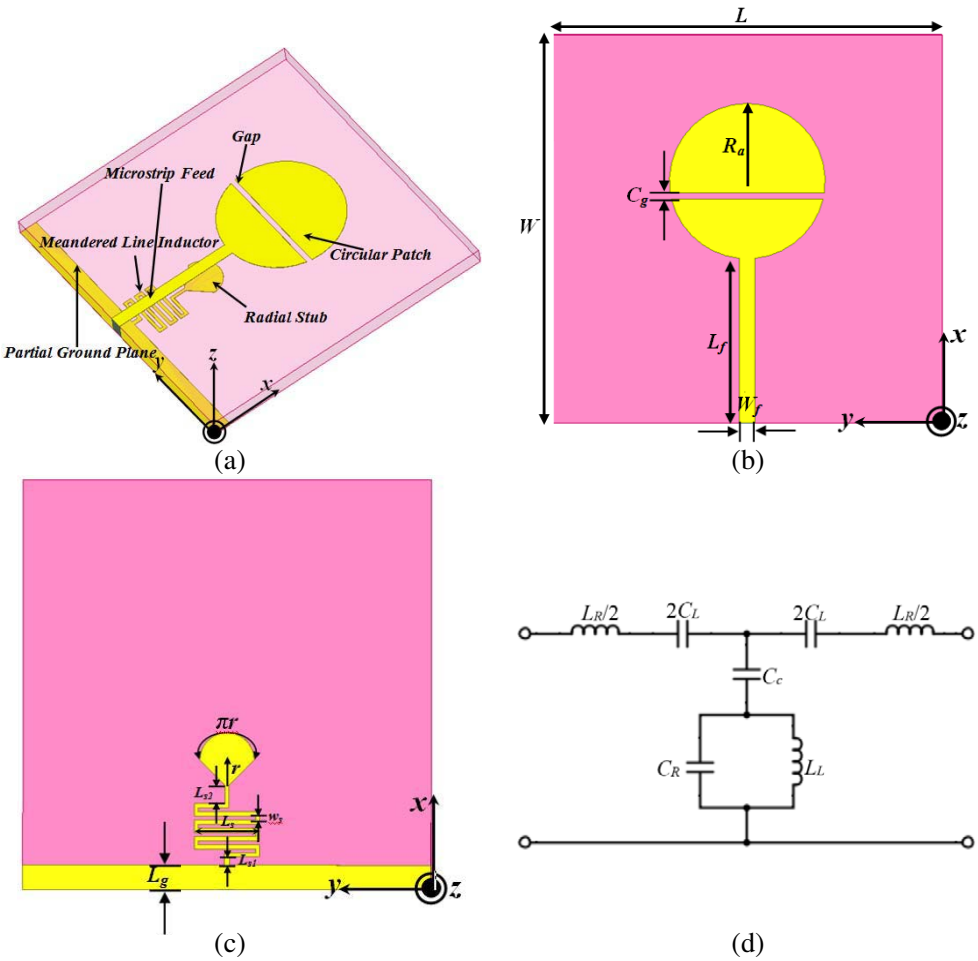

Figure 1. (a) Geometry of the proposed MTM antenna, (a) perspective view, (b) top view, (c) bottom view, (All dimensions are in mm: $L = 30$, $W = 30$, $L_f = 12.73$, $W_f = 1.2$, $C_g = 0.5$, $R_a = 6$ mm, $Lg = 1.8$, $r = 2$, $L_{s2} = 1.35$, $L_{s1} = 0.6$, $L_s = 4.8$, $W_s = 0.3$.), (d) equivalent circuit diagram of the proposed antenna.

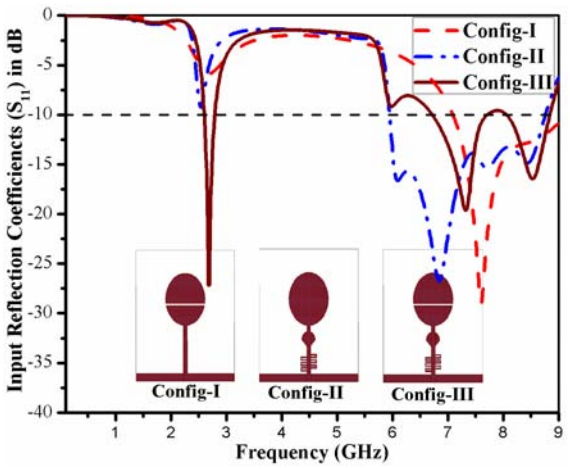

Figure 2. Input reflection coefficient of the proposed antenna for different configurations.

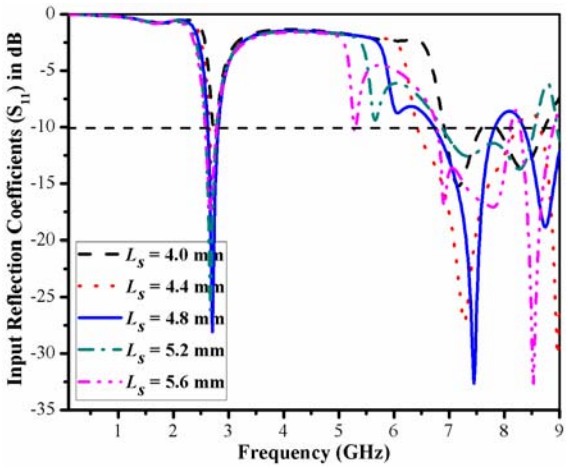

Figure 3. Input reflection coefficients of the proposed antenna by varying L_s.

5.95 GHz to 8.76 GHz due to the coupling between feed and ground plane. In order to improve the first mode, a series gap is introduced within the patch. As a result, the proposed antenna is capable to work in the 2.62–2.8 GHz band which leads to miniaturizing the electrical size of the antenna.

Next, input reflection coefficients are presented by varying some design dimensions specified in Fig. 1. which in turn is equivalent to the variation of lumped elements quantities. Fig. 3 shows the variation of input reflection coefficient on different values of L_S. Essentially this L_S deals with the shunt inductance present in the CRLH transmission line. It can be observed that it helps power to be transferred into the load for the first band. In addition, length of the meandered line inductors plays a prominent role on bandwidth of the second band as it affects the coupling between patch and ground plane.

Figure 4 deals with input reflection coefficients by varying radius of the radial stub (r). It can be observed that this parameter does not play a significant role to drive the frequency band; yet it is responsible for bandwidth of the second band.

The effect of series gap (C_g) is also discussed in Fig. 5. This study shows that there is not much role of this series gap to drive the lower order mode although it is important to have the series gap in order to complete the CRLH transmission line. It has already been established that for open-ended termination, the lower order mode can be tuned by shunt parameters rather than series parameters. Nevertheless, this parameter is responsible for tuning higher order band.

To reconfirm the validation of origination of modes, current distributions at 2.7 GHz and 7.34 GHz are plotted in Fig. 6 and Fig. 7, respectively. It can be observed from Fig. 6 that more current is

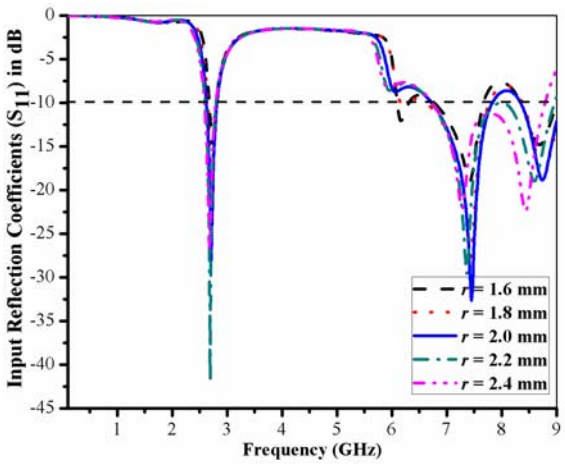

Figure 4. Input reflection coefficients of the proposed antenna by varying r.

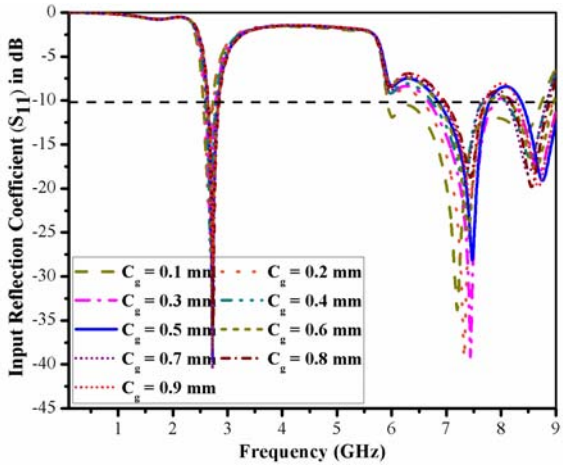

Figure 5. Input reflection coefficients of the proposed antenna by varying C_g.

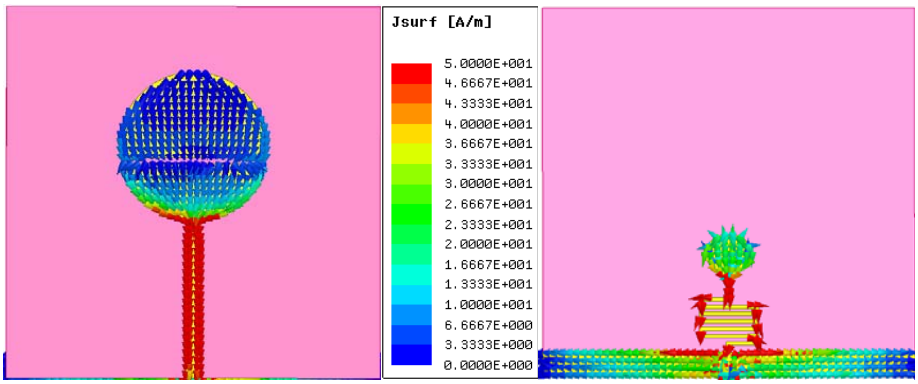

Figure 6. Current distribution of the proposed antenna at 2.7 GHz.

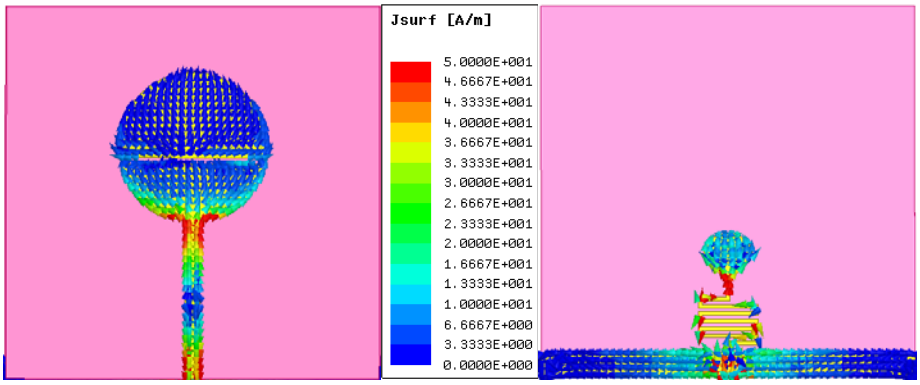

Figure 7. Current distribution of the proposed antenna at 7.34 GHz.

concentrated on feed and at fingers of the meandered line inductors. Therefore, it can be said that the contribution of meandered line inductor is prominent to originate this mode. On the other hand, Fig. 7 shows that the second band is due to the patch and ground plane. However, dimensions associated with the meandered line inductor and radial stubs affect the second band.

4. RESULTS AND DISCUSSION

The proposed antenna is fabricated on an FR4 Glass Epoxy substrate, and photographs of the fabricated prototype are displayed in Fig. 8. Input reflection coefficient was obtained experimentally by using Anritsu VNA Master MS 3028C. Fig. 9 shows comparison of the experimental input reflection coefficient results with the simulated one. Simulated results show two bands from 2.62 to 2.80 GHz and 6.57 GHz to 7.65 GHz with 6.6% ($f_c = 2.7$ GHz) and 14.57% ($f_c = 7.34$ GHz) fractional bandwidths respectively while measured results extend from 2.57 to 2.82 GHz (2.68 GHz) in the first band and 6.49 to 7.20 GHz (6.80 GHz) in the second band. It can be observed that measured results presents significant mismatch with the simulated ones in the second band. The major reason for this inconsistency is the fabrication tolerance and imperfect soldering. As can be seen in Fig. 8(b), there is a large amount of soldering wire pasted on partial ground plane which may affect the area covered by partial ground plane and consequently plays an important role in driving the second band.

Figure 10 shows the simulated and measured radiation properties of the proposed antenna at 2.7 GHz and 7.34 GHz, respectively. Figs. 10(a) and (b) depict dipolar type pattern in xz plane and omnidirectional pattern in yz plane with cross polarization level as below as -35 dB. On the other hand, Figs. 10(c) and (d) present some discontinuity in the pattern and deterioration at the 2nd mode (7.34 GHz). Good agreement between simulated and measured results can be observed in the lower band while some inconsistencies are involved in the higher band with the same trend. This may be due

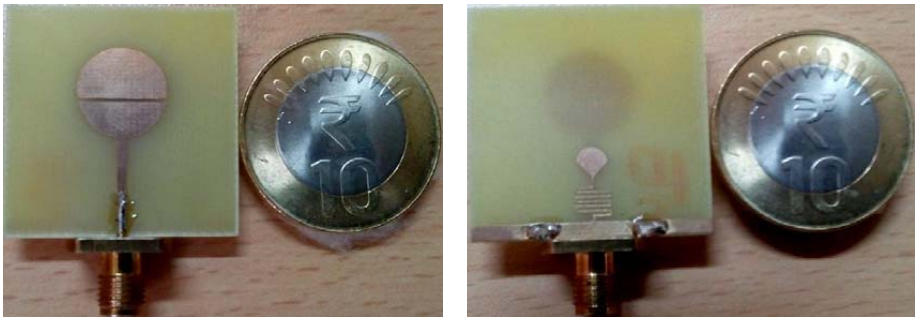

(a) Top view (b) Bottom view

Figure 8. Photograph of the fabricated prototype of the proposed antenna.

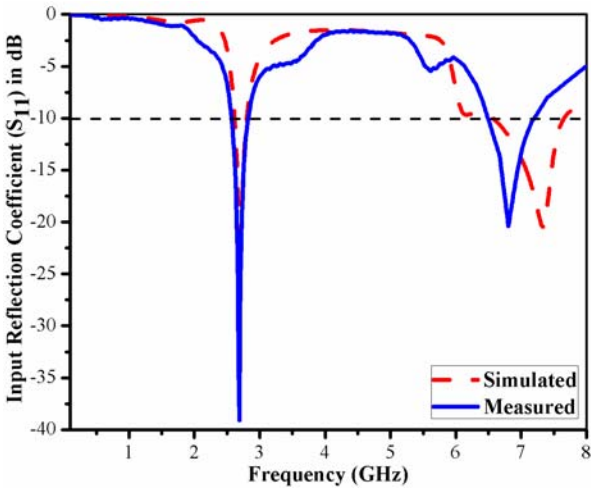

Figure 9. Simulated and measured input reflection coefficients of the proposed antenna.

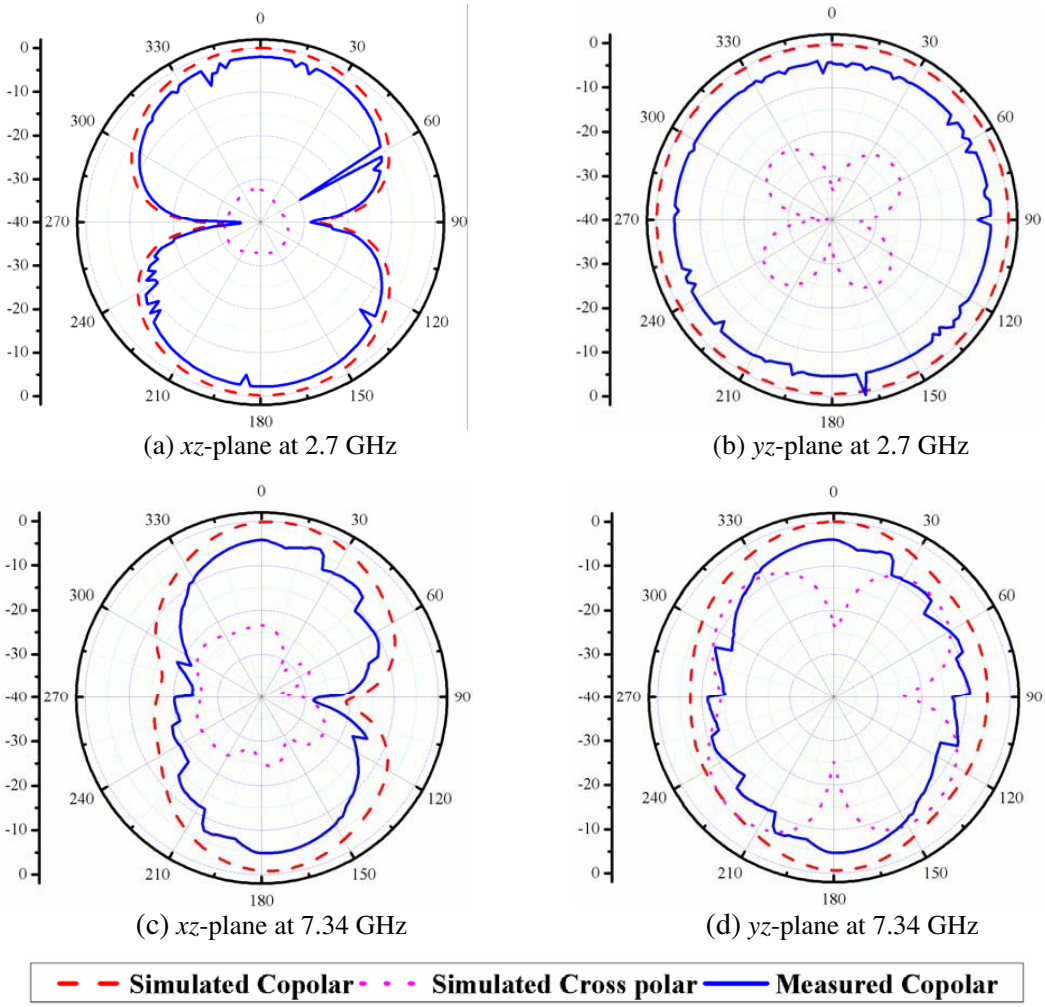

Figure 10. Simulated and measured radiation patterns of the proposed antenna.

to the high amount of loss incorporated in the higher frequencies.

The major advantage of this antenna is that it provides a reasonable gain even in the lower band as it offers 1.49 dB gain at 2.70 GHz in the boresight direction. In addition, the proposed antenna offers 3.23 dB simulated gain at 7.34 GHz. In general, metamaterial structures suffer from the low gain or negative gain problem in the lower bands [5, 14]. It is evident that at lower frequencies fields are tightly bounded on the surface of the structure due to high level of miniaturization [5]. Figs. 11(a) and (b) show peak gain results of the proposed antenna in the lower and higher bands, respectively.

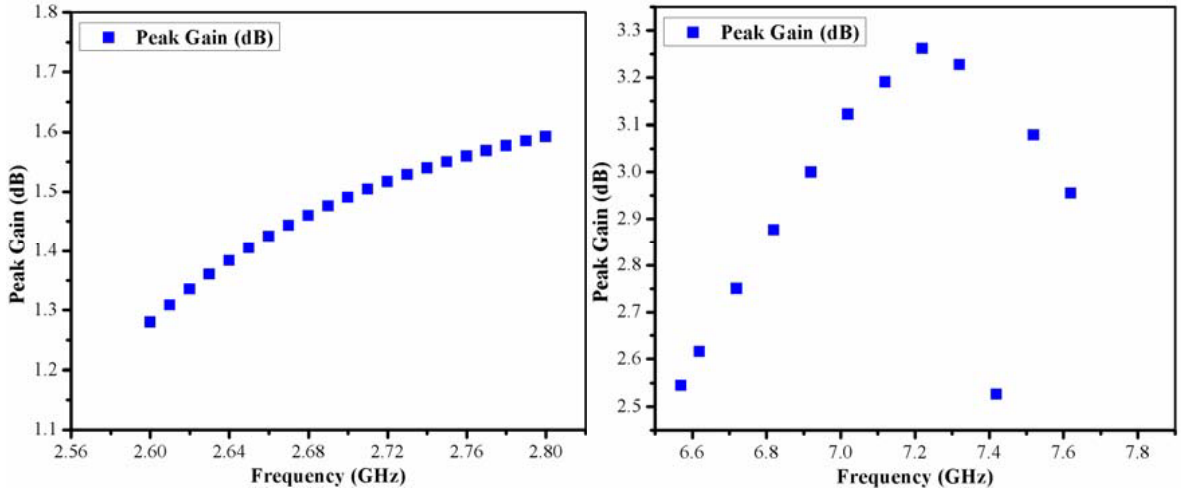

Figure 11. Simulated peak gain of proposed antenna, (a) at 2.60–2.80 GHz, (b) at 6.57–7.34 GHz.

Table 1 compares the proposed antenna with the metamaterial antennas published earlier. It is always a good practice to compare the electrical size of the antenna other than physical size of the antenna because it compares the physical size with respect to their resonant frequency. The proposed antenna is found more compact than the antennas published earlier except [14]. It can be seen from Table 1 that earlier published antenna structures experiencing negative gain problem consequently at this resonant frequency antenna will not be operational anymore. In addition, the proposed antenna has 6.6% fractional bandwidth which is comparable with that of others.

Table 1. Comparison of the proposed antenna with recent published work.

Parameters	**Proposed** work	**[5], 2014**	**[14], 2014**	**[16], 2015**	**[18], 2012**
Lowest order mode (f_r)	2.7	2.1	1.78	2.64	3.82
Electrical Size (λ_0)	0.27 × 0.27	-	0.11 × 0.11	0.26 × 0.17	0.50 × 0.44
Fractional Bandwidth (%)	6.6	0.66	3.08	3.8	6.8
Peak Gain (dBi)	1.49	−4.7	−0.15	2.74	3.85
Radiation Efficiency (%)	92.09	26.3	70	75.5	96
Via Process	Not Required	Yes	Not Required	Not Required	Not Required
Dielectric Constant (ε_r), loss tangent ($\tan\delta$)	4.4, 0.02	2.2, 0.0009	2.33, -	4.4, 0.02	2.1, 0.001
Thickness (mm)	1.6	1.57	0.508	1.6	1.57

5. CONCLUSION

A compact dual-band antenna based on CRLH-TL is designed and fabricated in this paper. It is demonstrated that virtual ground plane is beneficial in addition to partial ground plane, to realize a CRLH transmission line without enhancing the size of ground plane. This probably plays an eminent role to have perfectly omnidirectional pattern which is necessary for WiMAX, Bluetooth and WLAN/Wi-Fi applications. The proposed antenna has smaller electrical size of $0.27\lambda_0 \times 0.27\lambda_0 \times 0.014\lambda_0$ with 1.49 dB gain at 2.7 GHz, which is sufficient to integrate with mobile devices. Due to microstrip line based feeding, it is very easy to fabricate and analyze such structures.

ACKNOWLEDGMENT

The authors would like to thank Dr. M. K. Meshram, Associate Professor, IIT (BHU) Varanasi, India for providing lab facilities to measure S-parameters of proposed antenna.

REFERENCES

1. Alibakhshikenari, M., B. S. Virdee, A. Ali, and E. Limiti, "Miniaturised planar-patch antenna based on metamaterial L-shaped unit-cells for broadband portable microwave devices and multiband wireless communication systems," *IET Microwaves, Antennas & Propagation*, Vol. 12, No. 7, 1080–1086, 2018.
2. Al-Bawri, S. S., M. F. Jamlos, P. J. Soh, S. A. A. S. Junid, M. A. Jamlos, and A. Narbudowicz, "Multiband slot-loaded dipole antenna for WLAN and LTE-A applications," *IET Microwaves, Antennas & Propagation*, Vol. 12, No. 1, 63–68, 2018.
3. Zhang, T., R. L. Li, G. Jin, G. Wei, and M. M. Tentzeris, "A novel multiband planar antenna for GSM/UMTS/LTE/ZIGBEE/RFID mobile devices," *IEEE Transactions on Antennas and Propagation*, Vol. 59, No. 11, 4209–4214, 2011.
4. Anguera, J., C. Picher, A. Andújar, C. Puente, and S. Kahng, "Compact multiband antenna system for smartphone platforms," *7th European Conference on Antennas and Propagation (EuCAP)*, Gothenburg, Sweden, 2013.
5. Mehdipour, A., T. A. Denidni, and A.-R. Sebak, "Multi-band miniaturized antenna loaded by ZOR and CSRR metamaterial structures with monopolar radiation pattern," *IEEE Transactions on Antennas and Propagation*, Vol. 62, No. 2, 555–562, 2014.
6. Sharma, S. K. and R. K. Chaudhary, "A compact zeroth-order resonating wideband antenna with dual-band characteristics," *IEEE Antennas and Wireless Propagation Letters*, Vol. 14, 1670–1672, 2015.
7. Dadgarpour, A., B. Zarghooni, B. S. Virdee, and T. A. Denidni, "Beam tilting antenna using integrated metamaterial loading," *IEEE Transactions on Antennas and Propagation*, Vol. 62, No. 5, 2874–2879, 2014.
8. Li, D., Z. Szabó, X. Qing, E.-P. Li, and Z. N. Chen, "A high gain antenna with an optimized metamaterial inspired superstrate," *IEEE Transactions on Antennas and Propagation*, Vol. 60, No. 12, 6018–6023, 2012.
9. Caloz, C. and T. Itoh, *Electromagnetic Metamaterials: Transmission Line Theory and Microwave Applications*, John Wiley & Sons, Inc., U.S.A., ISBN 0-471-66985-7, 2006.
10. Sanada, A., C. Caloz, and T. Itoh, "Novel zeroth-order resonance in composite right/left-handed transmission line resonators," *Asia-Pacific Microwave Conference*, Vol. 3, 1588–1592, Seoul, Korea, 2003.
11. Lai, A., K. M. K. H. Leong, and T. Itoh, "Infinite wavelength resonant antennas with monopolar radiation pattern based on periodic structures," *IEEE Transactions on Antennas and Propagation*, Vol. 55, No. 3, 868–876, 2007.

12. Jang, T., J. Choi, and S. Lim, "Compact coplanar waveguide (CPW)-fed zerothorder resonant antennas with extended bandwidth and high efficiency on vialess single layer," *IEEE Transactions on Antennas and Propagation*, Vol. 59, No. 2, 363–372, 2011.
13. Niu, B.-J., Q.-Y. Feng, and P.-L. Shu, "Epsilon negative zeroth- and first order resonant antennas with extended bandwidth and high efficiency," *IEEE Transactions on Antennas and Propagation*, Vol. 61, No. 12, 5878–5884, 2013.
14. Amani, N., M. Kamyab, A. Jafargholi, A. Hosseinbeig, and J. S. Meiguni, "Compact tri-band metamaterial-inspired antenna based on CRLH resonant structures," *Electronics Letters*, Vol. 50, No. 12, 847–848, 2014.
15. Huang, H., Y. Liu, S. Zhang, and S. Gong, "Multiband metamaterial-loaded monopole antenna for WLAN/WiMAX applications," *IEEE Antennas and Wireless Propagation Letters*, Vol. 14, 662–665, 2015.
16. Gupta, A. and R. K. Chaudhary, "A compact short-ended zor antenna with gain enhancement using EBG loading," *Microwave and Optical Technology Letters (MOTL)*, Vol. 58, 1194–1197, 2016.
17. Li, D., Z. Szabó, X. Qing, E. P. Li, and Z. N. Chen, "A high gain antenna with an optimized metamaterial inspired superstrate," *IEEE Transactions on Antennas and Propagation*, Vol. 60, No. 12, 6018–6023, 2012.
18. Ha, J., K. Kwon, Y. Lee, and J. Choi, "Hybrid mode wideband patch antenna loaded with a planar metamaterial unit cell," *IEEE Transactions on Antennas and Propagation*, Vol. 60, No. 2, 1143–1147, 2012.